Effect of the MMA Content on the Emulsion Polymerization Process and Adhesive Properties of Poly(BA-*co*-MMA-*co*-AA) Latexes

Hongping Xu,[1] Nongyue Wang,[2] Taoguang Qu,[3] Jianguang Yang,[2] Yanmei Yao,[2] Xiongwei Qu,[2] Peter A. Lovell[4]

[1]*Hangzhou City Xiaoshan District Technical School, Xiaoshan, 311201, People's Republic of China*
[2]*Institute of Polymer Science and Engineering, School of Chemical Engineering, Hebei University of Technology, Tianjin, 300130, People's Republic of China*
[3]*College of Chemistry, Chemical Engineering and Materials Science, Suzhou University, Suzhou, 215123, People's Republic of China*
[4]*Macromolecular Group, School of Materials, The University of Manchester, Manchester M1 7HS, United Kingdom*

Received 7 April 2010; accepted 25 March 2011
DOI 10.1002/app.34572
Published online 9 August 2011 in Wiley Online Library (wileyonlinelibrary.com).

ABSTRACT: In the past work, the shear resistance of pure poly(*n*-butyl acrylate) was low, even incorporation of inorganic filler, silica in the composition. It is well-known that the copolymerization of *n*-butyl acrylate (BA) with methyl methacrylate (MMA) will increase the glass transition temperature, and enhance the shear resistance of acrylic polymers. In the current work, the preparation of a series of acrylic water-borne pressure-sensitive adhesives (PSAs) with the controlled composition and structure for the copolymerization of BA and acrylic acid (AA) with different MMA contents, poly(BA-*co*-MMA-*co*-AA) was reported and its effects on adhesive properties of the latices were investigated. The latices of poly(BA-*co*-MMA-*co*-AA) were prepared at a solid content of 50% by two-stage sequential emulsion polymerization, and this process consisted of a batch seed stage giving a particle diameter of 111 nm, which was then grown by the semicontinuous addition of monomers to final diameter of 303 nm. Dynamic light scattering (DLS) was used to monitor the particle diameters and proved that no new nucleation occurred during the growth stage. Copolymerization of BA with MMA raised the glass transition temperature (T_g) of the soft acrylic polymers, and had the effect of improving shear resistance, while the loop tack and peel adhesion kept relatively high. The relationship between pressure-sensitive properties and molecular parameters, such as gel content and molecular weight, was evaluated. © 2011 Wiley Periodicals, Inc. J Appl Polym Sci 123: 1068–1078, 2012

Key words: adhesives; dynamic light scattering; emulsion polymerization; size exclusion chromatography (SEC); structure–property relations

INTRODUCTION

Pressure-sensitive adhesives (PSAs) are viscoelastic materials that can adhere strongly to solid surfaces upon application of light contact pressure for a short contact time.[1] Emulsion polymerization as a technology for PSA production offers better environmental compliance compared to solvent technology and better energy efficiency compared to hot-melt technology. Polyacrylates are transparent and colorless, and because they are saturated, they are very resistant to oxidation and do not yellow on exposure to sunlight. Emulsion acrylic copolymers have enjoyed the fastest growth and the biggest share of the PSA market in commercial applications.[2,3] Among acrylic polymers making for PSAs, long-alkyl acrylates, such as poly(*n*-butyl acrylate), poly(BA),[4–15] and poly(2-ethyl hexyl acrylate), poly(2-EHA)[2,4,15–21] are generally used. However, because these kinds of acrylic PSAs comprise polymers that have high entanglement molecular weight (M_e) values,[22] low glass-transition temperature (T_g) values, and medium to low molecular weights, this may present a problem in PSA label converting and high temperature printing, and some types of crosslinking must be provided to yield shear holding power.[15,22–26] It is for such reasons that homopolymers are rarely

Correspondence to: X. Qu (xwqu@hebut.edu.cn).
Contract grant sponsor: Natural Science Foundation of Hebei Province; contract grant number: E2010000107.
Contract grant sponsor: Key Lab for Nanomaterials, Ministry of Education; contract grant number: 2007-2.
Contract grant sponsor: Excellent Project of Ministry of Personal Resources of China; contract grant number: 2006-164.
Contract grant sponsor: Ministry of Education of China; contract grant number: 2007-24.
Contract grant sponsor: Key Lab of Beijing City on Preparation and Processing of Novel Polymer Materials; contract grant number: 2006-1.
Contract grant sponsor: Distinguished Youth Scientist of NSF; contract grant number: 50725310.

used for pressure-sensitive adhesive applications, although intraparticle crosslinking occurs as part of the chain transfer to the polymer during emulsion polymerization.[27,28] A balanced combination of tack, peel strength, and shear resistance is of primary concern in PSA production. To achieve this purpose, a PSA is usually a copolymer of an inherently tacky polymer (used to provide adhesion) with a higher T_g polymer used to increase modulus. Copolymerization of acrylic ester with other monomers, such as methyl methacrylate (MMA),[2,7,9–14,16–21] styrene (St),[1,6,29] and vinyl acetate (VAc)[4,8] is used to vary the chemical and physical properties of the adhesives. However, the increase in polymer modulus by the inclusion of higher T_g polymer is often at the expense of the essential adhesion properties. Generally the amount of modulus-enhancing monomer used for such purposes is usually small to minimize the loss in tack of the polymer.

In the past work, the shear resistance of poly(*n*-butyl acrylate) was low,[30] even incorporation of inorganic filler, silica,[31] and chain transfer agent, CTA in the compositions.[5,32,33] It is well-known that the copolymerization of BA with MMA will increase the glass transition temperature, and enhance the shear resistance of acrylic polymers.[7,9–14,34] In spite of their commercial importance, less work has been dedicated to systematically synthesize the controlled composition and structure for the copolymerization of BA with different MMA contents by semicontinuous emulsion polymerization and influence of the composition on the adhesive properties of PSAs.[9,11,14,35–37] In this study, we focused on investigation of the semicontinuous emulsion polymerization of BA and acrylic acid (AA) with different contents of MMA monomer between 0 and 30% on the basis of the second-growth acrylic monomers' weight. The effects of the addition of MMA on the gel fraction, entanglement molecular weight (M_e), and soluble molecular weight of poly(BA-*co*-MMA-*co*-AA) were studied. Adhesive properties were related to the adhesive performance, such as loop tack, peel force, and shear resistance.

EXPERIMENTAL

Materials

The initiator potassium persulfate (KPS) was obtained from Tianjin Chemistry Agent (Tianjin, China). The anionic surfactant used in this study was Aerosol Series from Cytec, (Hevens, Netherlands) Tert-dodecylmercaptan (TDM) was obtained from Merck-Schuchardt (Hohenbrunn, Germany). All these materials were used without further purification. BA, AA, and MMA were commercial grade and were available from Beijing Dongfang Chemical (Beijing, China). BA monomer was first washed three times with a 2% NaOH solution, then washed with deionized water until the washed waters were neutral, and finally dried with $CaCl_2$ overnight, after which it was distilled under reduced pressure. AA and MMA were distilled under reduced pressure before use. Hydroquinone (99%) was used as an inhibitor of the latices taken from the emulsion polymerization procedure. Tetrahydrofuran (THF) (HPLC grade, Tianjin) was used in the molecular weight determination. Deionized water was used throughout the study.

Semicontinuous emulsion polymerization process

PSAs were prepared as 50 wt % solid lattices by semicontinuous emulsion polymerization involving two sequential stages. The first seed stage involved the formation of seed particles of 111 nm in diameter with a batch process. This was followed by the second growth stage, which took the final particle diameter of 300 nm. In the second growth stage, different MMA contents were added to the polymerization system with semicontinuous emulsion polymerization. The surfactant (2.5 g) and water (700.0 g) were added to a 3-L flanged reaction flask. The flow of nitrogen was begun and the water batch temperature was attained at 78°C. During the following 20 min, the seed stage BA monomer (50.0 g, 5 wt % of total monomer) was added to the surfactant solution and stirred for 10 min before KPS (2.15 g) dissolved in water (100.0 g) was added to start the reaction. The seed stage was 60 min. In the growth stage, the preemulsified monomer mixture of BA (922.65–645.85 g), acrylic acid (AA, 27.35 g), and MMA (0–276.80 g, accounting for 0, 6, 12, 18, 24, and 30%, respectively, on the basis of the second-growth acrylic monomers' weight) with surfactant (11.88 g) and TDM (0.333 g) were dropped into the flask using a Watson-Marlow peristaltic pump (Model 505S) at a constant rate over 3 h. KPS (0.215 g) dissolved in water (50.0 g) was added to the reaction flask at 115, 175, and 235 min. After the completion of the addition of the growth-stage reactant mixture, a further 60 min was allowed before the latex was cooled to room temperature and filtered through a 53-μm sieve to obtain the coagulate content. Residual monomers were measured with gas chromatograph/mass spectrometer (GC/MS) and were less than 0.5% on the basis of the wet latex weight.

Conversion and particle diameter measurement of the latices

At 30-min intervals, samples of the latex (10 mL) were removed into preweighed vials containing 1 g hydroquinone solution (5 wt %) to prevent the

further polymerization, and were immediately placed in an ice-bath to short stop the reaction, then analyzed gravimetrically to determine the instantaneous conversion (on the basis of the monomer fed until the sampling time) and overall conversion (on the basis of the monomer fed in the full emulsion polymerization process). Particle sizes were measured at 633 nm with a fixed 90° scattering angle with dynamic light scattering (DLS) on a Malvern Zetasizer 3000HS (Worcestershire, UK) and the cell temperature was controlled at 25°C ± 0.1°C. The particle diameters quoted are the mean values of the *z*-average diameters (d_z's) calculated by the cumulant method. The reported polydispersity index values (PDI) were those given by the instrument and were not conventional PDI values. They are referred to as Malvern Polydispersity Index (M-PI) throughout this work to avoid any misunderstanding. A value closer to 0.01 indicates a narrower distribution.

Solvent extraction and molecular weight characterizations

The soluble polymer fractions were separated from poly(BA-*co*-MMA-*co*-AA) copolymers by extraction of the dried lattices with boiling tetrahydrofuran (THF) for 2 days by means of Soxhlet extraction. The insoluble polymers left in the thimble were dried in a vacuum oven at 70°C for 36 h to obtain the gel content, which was determined by the difference in weight of the sample before and after solvent extraction. Each analysis was performed in duplicate and the results reported were the averages. The soluble molecular weight of the polymer collected by the THF extraction was determined by size exclusion chromatography (SEC) with the apparatus (Waters 515, Milford, MA) equipped with refractive-index detector (Waters 2410) and data system (Millennium 32). Filters were placed before the columns to prevent gel damage to the column. The temperature was kept constant at 38°C on both detector and column. THF was used as the solvent at a flow rate of 1.0 mL min^{-1}. The molecular weight of the sample was calculated using the conventional calibration technique with polystyrene standards to get relative molecular weight.

Dynamic mechanical analysis

Dynamic mechanical properties, including the storage modulus (G′) and damping factor (tan δ) of poly(BA-*co*-MMA-*co*-AA), were obtained with a Triton 2000 (Keyworth, UK) dynamic mechanical analyzer in plate clamp mode. The plate sample with typical dimensions of 10 × 5 × 2 mm^3 was prepared through cast molding. The heating rate and frequency were 5°C min^{-1} and 1 Hz, respectively. Glass transition temperatures (T_g's) were located from the peaks in the loss tangent.

PSA testing

The lattices prepared were adjusted to pH 5.5 with a 25 wt % ammonia solution and filtered again. After that, they were coated with a Elcometer (Manchester, UK) 4360/15 bar onto 36 μm thickness poly(ethylene terephthalate) to give a film with a dry thickness of 30 μm and dried in a fan-assisted oven at 105°C for 4 min. Adhesive bonds were formed by the application of a standard 2-kg roller passing over twice. All adhesive testing was performed at 23°C and 50% relative humidity, and the samples were seasoned at these conditions for 24 h before measurements. Loop tack and 180° peel were done off a stainless steel substrate. Test methods were in accordance with the FINAT test methods No. 9 and 1 at 300 mm min^{-1}. Shear resistance was done off a glass plate substrate with a 25 × 25 mm^2 poly(ethylene terephthalate) coated strip and a 1000-g hanging weight according to FINAT test method No. 8. The time to failure was recorded. The average values were from three trials.

RESULTS AND DISCUSSION

Latex preparations

Lattices were prepared with seeded emulsion polymerization, that is, the addition of monomer, initiator, and surfactant to a previously prepared latex, which had the advantage of preventing the uncertainties of the particle initiation stage and, therefore gave better batch-to-batch reproducibility. Instantaneous and overall conversions were calculated from a mass balance of the reagents in the polymerization with the solid content measured at each sampling time.

$$\text{Instantaneous percentage conversion}(\%) = \left(\frac{\text{mass of polymer formed}}{\text{mass of monomer added}}\right) \times 100$$

where the mass of monomer added is the sum of the monomer in the seeded stage and any monomer that has been added during the growth stage;

$$\text{Overall percentage conversion}(\%) = \left(\frac{\text{mass of polymer formed}}{\text{total mass of monomer}}\right) \times 100$$

where the total mass of monomer is the sum of the monomer in the seed stage and all the monomer in the growth stage.

Plots of conversion versus reaction time for the typical latex preparations are shown in Figure 1

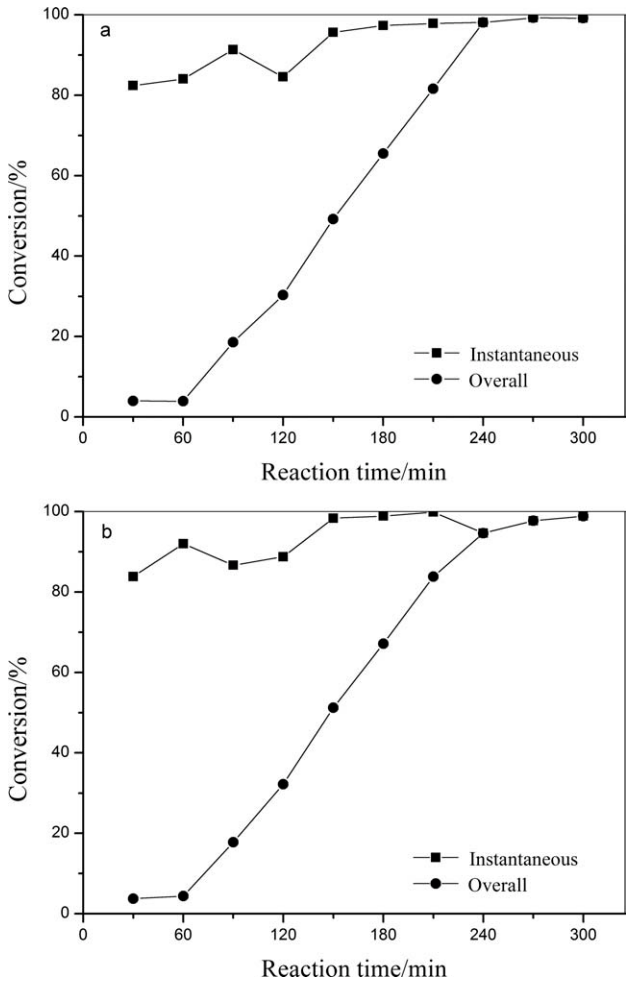

Figure 1 Variation of the instantaneous and overall percentage conversions with the reaction time with different MMA contents: (a) 0%, (b) 30%.

with the addition of MMA content of 0 and 30%. The reason for this choice is the large differences in the solubilities of the BA and MMA monomers in the aqueous phase, 15 g L^{-1} for MMA and 2 g L^{-1} for BA.[9] The main monomers (BA and MMA) used to prepare the lattices have very different reactivity ratios[38] ($r_{MMA} = 2.24$ and $r_{BA} = 0.414$), so it is possible to obtain a heterogeneous copolymer composition.[4] To control the distribution of MMA and BA units in the polymer chains as well as in the polymer particles, it is first necessary to establish the starved feed conditions. The polymerizations were observed to proceed at high instantaneous conversion (>80%). High conversion was maintained during the addition step to prevent secondary particle nucleation. This was an important aspect of the polymerization for the control of particle's composition and morphology. Final overall conversions were found to be high (>97%) for all polymerizations, which showed that a continuation of the polymerization for 1 h after the end of the monomer addition was adequate to allow for complete conversion. Table I summarizes the results of the emulsion polymerization procedure with different MMA levels. It can be seen that the final conversion slightly decreased with the MMA content, that is, the higher the amount of MMA, the lower was the conversion at a certain point in time, which was due to the fact that the propagation rate coefficient for BA was an order of magnitude higher than it is for MMA.[11]

DLS technique is used to obtain quantitative information about the particle sizes of colloidal systems. In this study, DLS provided a rapid means of monitoring the particle size of the lattices during both the seeded and growth stages of the polymerization. With this information, it was possible not only to establish and reproduce a latex system of the known particle diameter but also to determine whether, during the growth stage of the polymerization, the latex particles grew sequentially or if the secondary nucleation occurred.

Latex particle diameters are determined by DLS and compared with those theoretically calculated from the following equation[39]:

$$d_t = \left(\frac{M_t I_t}{M_s}\right)^{1/3} \times d_s$$

where d_t is the diameter of the latex particle at time t, M_t is total mass of monomer added at time t, I_t is instantaneous conversion, M_s is mass of monomer added in the seed stage, and d_s is the seed particle diameter as measured by DLS. Plots of the particle diameter versus reaction time for the typical latex preparations are shown in Figure 2 with the addition

TABLE I
Some Parameters of the Final Data for the Poly(BA-*co*-MMA-*co*-AA) Latexes with Different MMA Contents

MMA content (wt %)	Final particle diameter (nm)	Polydispersity index of the final latex	Overall conversion (wt %)	Coagulate content (wt %)
0	306	0.0113	99.2	0.29
6	303	0.0301	98.8	0.31
12	300	0.0424	98.3	0.26
18	305	0.0228	97.8	0.32
24	305	0.0200	97.4	0.36
30	306	0.0020	97.1	0.41

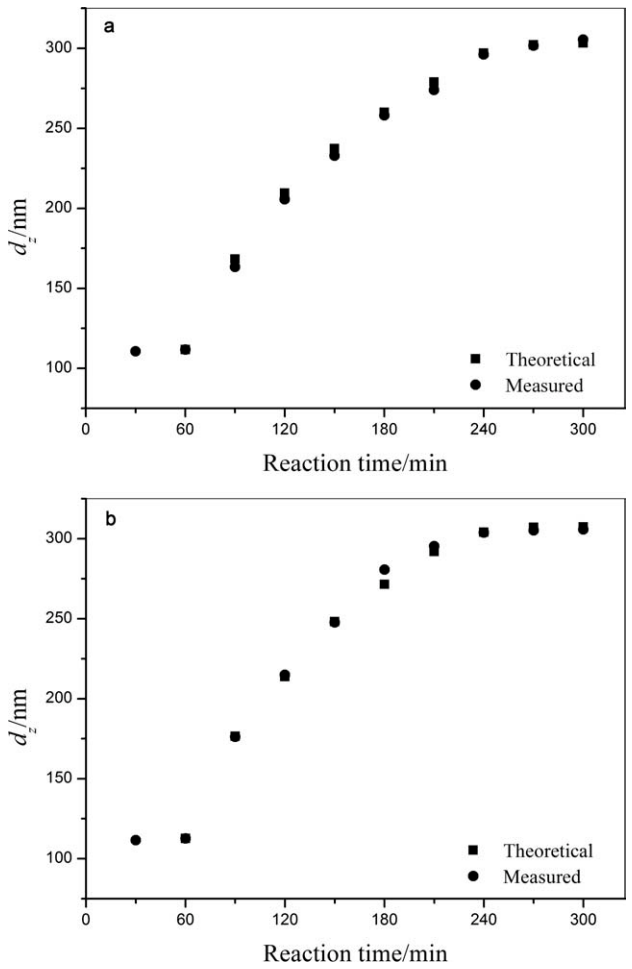

Figure 2 Variation of the measured and theoretical d_z with the reaction time with different MMA contents: (a) 0%, (b) 30%.

of MMA contents of 0 and 30%. The good agreement shown between experimental and theoretical particle diameters throughout the polymerization for the lattices provided strong evidence that the observed particles were grown without significant secondary nucleation and that the latex particles formed were spherical. This, coupled with the low levels of coagulum (<0.5 wt %) measured for the lattices, showed that the correct surfactant concentration was used in the growth stage of the polymerization. The solid contents for all of the lattices were nearly 50 wt %, with the final particle diameters of 303 ± 3 nm, listed in Table I. The particle sizes for all of the lattices were almost the same within the experimental error at different levels of MMA content, and the colloidal stability of the lattices was not affected because the coagulate contents for these six latex preparations were low. Therefore, the presence of hard monomer (MMA) had no significant effect on the final monomer conversion and the particle size in the semicontinuous emulsion polymerization. Meanwhile, different chemical composition distributions can be obtained because of the difference in reactivity of the two monomers,[38] but the semicontinuous polymerization ran under well-starved conditions could avoid the accumulation of BA, that is, the rate of addition of the monomers is slower than is the rate of reaction. In conclusion, the instantaneous composition of polymer particles is close to that of the feed at every moment, and the polymerization process can control the composition and structure of the polymer particles.

Molecular characterization

Transitional behavior

Dynamic mechanical analysis (DMA) is a sensitive thermal analytical technique for detecting transitions associated with molecular motions within polymers in the bulk state. To confirm the proposed structures, DMA analyses were conducted to evaluate the T_g values resulting from the copolymerizations of BA and AA with various MMA contents. In Figure 3, the dynamic mechanical spectra of the films cast

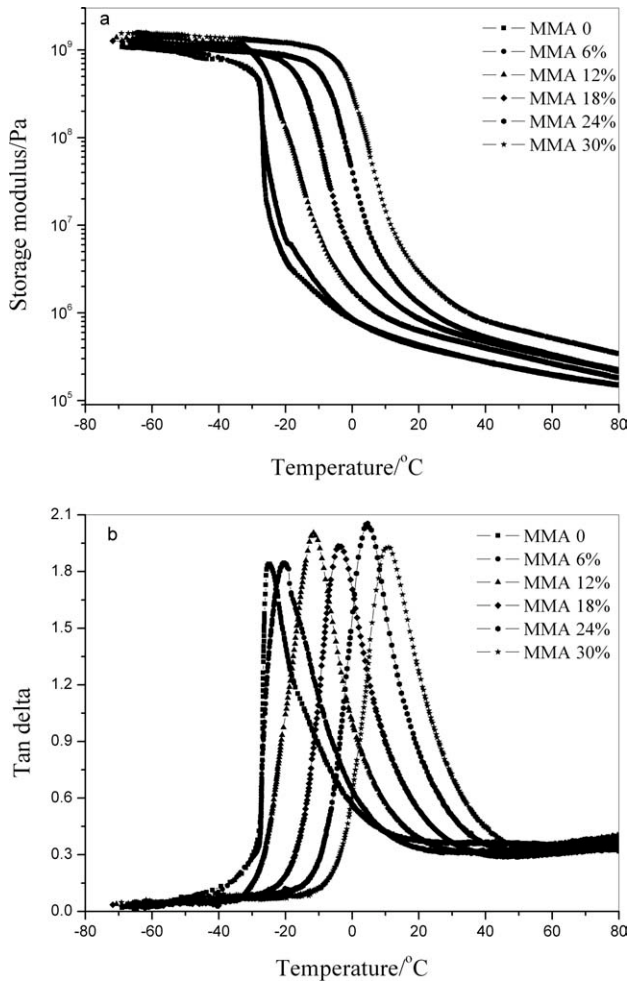

Figure 3 Curves of (a) G' and (b) tan δ versus the temperature of the PSA polymers with different MMA contents.

TABLE II
Values of T_g and M_e of the Poly(BA-*co*-MMA-*co*-AA) Copolymers with Different MMA Contents

MMA content (%)	0	6	12	18	24	30
T_g (°C)	−24.4	−19.7	−11.6	−3.7	4.7	10.9
M_e (kg mol^{-1})	22.2	21.3	20.3	20.2	20.2	17.1

from the lattices show a single T_g for each polymer, proving that the copolymers have a homogeneous composition. The width of the glass transition could be related to the properties of these polymers. A simple sharp transition occurred in the tan δ at the glass transition temperature for low MMA contents. Semicontinuous emulsion process where the monomer(s) is continuously fed into the reaction medium containing pre-existing particles and polymerized is a good tool for minimizing the deviation of the copolymer composition from that of the comonomers. As the MMA contents increases, Figure 3 shows that the transition regions are slightly broader than those observed from the low MMA contents. The reason was the differences of the monomers' reactivity ratios.[38] The glass transition temperatures of the poly(BA-*co*-MMA-*co*-AA) polymers with different MMA contents in the growth stage are given in Table II. It can be seen that the T_g increases with the increasing amount of MMA comonomer as expected. In fact, the T_gs of the respective polymers linearly increase with the increasing amount of MMA comonomer, shown in Figure 4, which also indicates that the statistical copolymers are synthesized. It appears that the addition of a high T_g comonomer obviously increases the T_g value of the copolymer.

Gel content

The coagulated samples were obtained by freeze-thaw cycling, and washed with deionized water several times. After the samples were dried, the gel contents of poly(BA-*co*-MMA-*co*-AA) copolymers were determined by Soxhlet extraction. The gel was arisen from termination by the coupling of propagating long-chain branches formed by intermolecular chain transfer to polymer.[27] Figure 5 shows the values for the gel fraction at different MMA contents. According to the previous results, the emulsion polymerization of poly(BA-*co*-MMA-*co*-AA) lattices prepared was run under monomer-starved conditions. Thus, the polymer concentration in the latex particles was high at all times, and as a result, microgels were formed early. As the reaction proceeded, the formation of microgels increased.[39] This was expected because higher molecular weight species were the most prone for hydrogen abstraction and chain transfer because of higher number of tertiary carbon atoms per chain.[40] As the structure in methyl methacrylate (MMA) molecule does not contain tertiary carbon atoms, the higher MMA content is, the lower is the gel fraction. With the addition of 30 wt % MMA in the composition in the growth stage, gel fraction was almost completely avoided. Therefore, the gel fraction significantly decreased with the increase of MMA content, as shown in Figure 5.

Molecular weight

Table III presents the evolution of the soluble polymer molecular weights and their distributions. The final soluble polymer molecular weight slightly increased as the amount of the MMA used in the

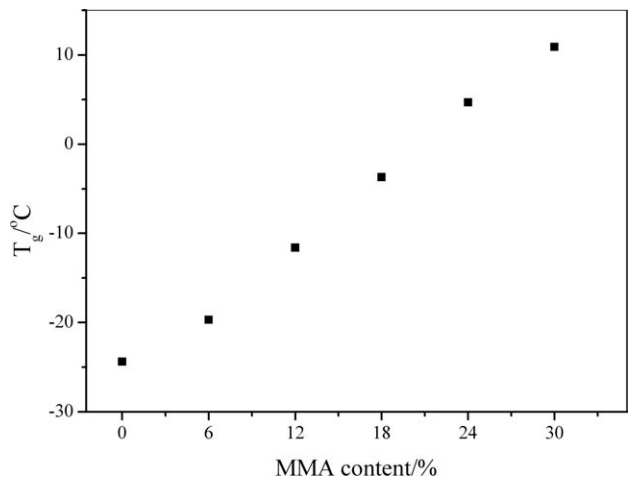

Figure 4 The relationship between T_g and MMA content.

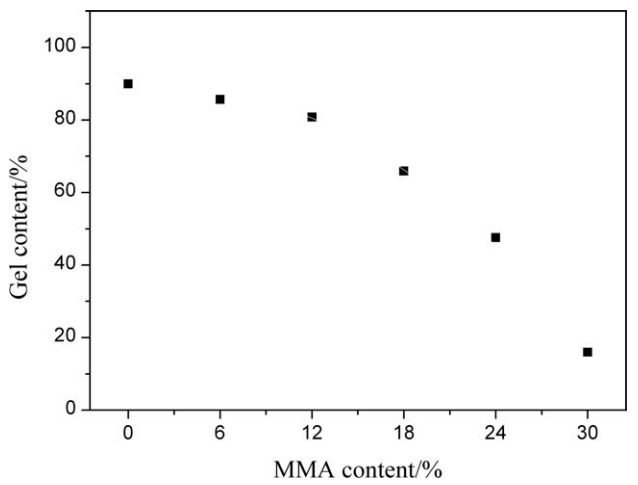

Figure 5 Variation of the gel content with the MMA content.

TABLE III
Summary of the Molecular Weights of the Soluble Poly(BA-*co*-MMA-*co*-AA)

MMA content (%)	M_n (kg mol^{-1})	M_w (kg mol^{-1})	MWD
0	92.5	286.5	3.1
6	110.5	501.1	4.5
12	115.8	543.0	4.7
18	121.3	533.7	4.4
24	123.8	547.0	4.5
30	125.4	567.5	4.5

experiment increased, while the MMA content had no significant effect on the soluble molecular weight distribution (MWD). The raw data (detector signal versus elution time) are used to compare the molecular weight distributions of the different lattices, shown in Figure 6. In the experiments carried out without and with low MMA contents, the increase of the soluble polymer molecular weight was because the transfer reaction from the soluble fraction to the gel of large and branched polymer chains was lower, formed by tertiary carbon's hydrogen abstraction to the polymer plus termination by combination reactions. On the contrary, in the experiments carried out with high amounts of the MMA contents, the increase in molecular weight was mainly due to the increase in the kinetic chain length by MMA propagation reaction,[38] so the chain transfer of large molecules from the soluble fraction to the gel was not significant. These results were consistent with those of Asua that copolymerization of BA with MMA led to a decrease of the gel fraction for increasing concentration of MMA, and the sol molecular weight increased with the MMA concentration.[37] In fact, the molecular weight values reported in Table III cannot be taken as the actual values, but they are useful for comparison purposes.

Another utility of DMA data is to determine entanglement molecular weight (M_e). M_e can be estimated from rubbery plateau modulus (G_N^o) shown as follows:

$$M_e = \frac{\rho_p RT}{G_N^o}$$

where ρ_p is density of the polymer, R is 8.31×10^7 dyne-cm/mol K, T is absolute temperature where G_N^o is located, and G_N^o is determined from G' at the onset of rubbery region (usually where tan δ reaches minimum following the prominent maximum). For crosslinked PSA, it is determined as a point of inflection in tan δ curve following the prominent maximum. The results of M_e values are listed in Table II also. Emulsion polymerization of low-T_g acrylics (BA) carried out to complete conversion produced a significant amount of microgels inside the particles due to chain transfer to the polymer via the hydrogen abstraction of tertiary vinyl carbons.[11] The gel content decreased, while the molecular weight of the soluble polymers increased with the MMA content. As the sol molecular weight of poly(BA-*co*-MMA-*co*-AA) was large enough, the microgels still could entangle with the soluble polymer chains, which, in turn, could entangle with other chain ends from another particle after film formation. The overall results were that the molecular weight between entanglements, M_e values for the poly(BA-*co*-MMA-*co*-AA) decreased with the increase of MMA monomer.

Adhesive properties

The adhesive testing results are shown in Figure 7. Increasing the MMA content in the second growth stage from 0 to 30 wt % in the copolymer of poly(BA-*co*-MMA-*co*-AA) served to decrease the loop tack force and peel strength, but significantly increase the shear resistance, over 100,000 min at 18 and 24 wt % MMA contents.

Surface force interactions play an important role in PSA bonds. The adsorption of the adhesive molecules onto the adherent surfaces occurs mainly by physical adsorption. In physical adsorption, the attractive forces for the adhesive molecule to the adherent surface are secondary to Van der Waal's force. Yang[41] found that for polyacrylic samples, the surface tensions were in the range between 31 and 37 dyn cm^{-1}. Because the surface tension of the stainless steel is 44 dyn cm^{-1}, we can expect good wetting to be achieved for all samples. Thus, PSAs need the polymers to be soft, capable of wetting the adherent surface and capable of sufficient cold flow to fill the surface irregularities.

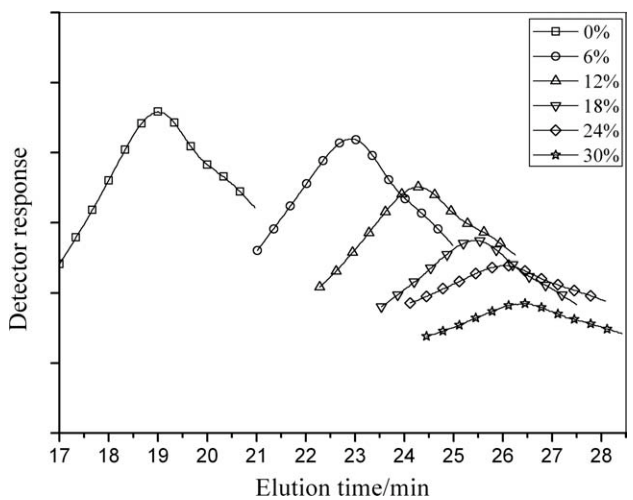

Figure 6 SEC chromatograms of the soluble polymer fraction of the dried latices with different MMA contents, (a) 0%, (b) 6%, (c) 12%, (d) 18%, (e) 24%, (f) 30%.

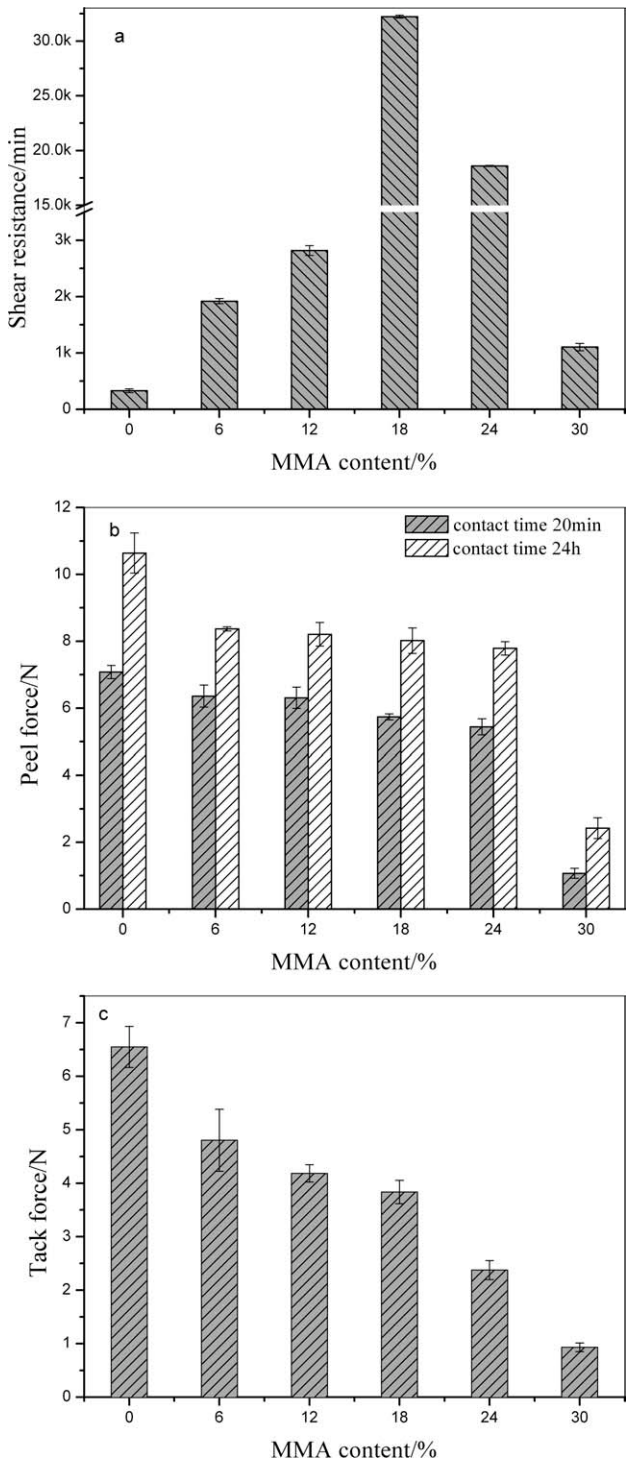

Figure 7 Effects of the MMA content on the adhesive properties: (a) shear resistance, (b) peel force, (c) loop tack.

The shear resistance of an adhesive is that which resists the tendency to flow or creep. This property is of great importance in PSA applications. The mechanism of bond failure must be in the bulk of the adhesive and not at the interface for the test to be a measure of cohesive strength. As shown in Figure 7(a), coated pressure-sensitive adhesives show dramatic increase in shear resistance as the MMA content increases, with the mode of failure being cohesive for all tests. Shear resistance was a measure of the cohesive strength of an adhesive and as such was related to the mobility of the polymer chains. Emulsion polymerization of BA monomer carried out to complete conversion produced significant amount of microgels inside the particles due to chain transfer to polymer via hydrogen abstraction of tertiary vinyl carbons.[27] As MMA monomer does not contain tertiary vinyl carbons, the gel content will decrease with the increase of the MMA content, shown in Figure 5. An increase from 0 to 18% MMA content in the growth stage of the mixture of BA, MMA and AA monomers resulted in an increase in T_g of $\sim 16^{\circ}$C. An increase from 18 to 30% MMA content produces a further increase in T_g of $\sim 12^{\circ}$C, as listed in Table II. It can be seen that as the quantity of MMA content in the growth stage polymerization increased from 0 to 18% an increase in shear resistance from 330 to 32,240 min was observed. The most important factor was the increase in polymer T_g as a consequence of the increased quantity of MMA. A rise in T_g toward the testing temperature caused a reduction in polymer chain mobility and hence an increase in shear resistance. However, poly(BA-*co*-MMA-*co*-AA) copolymers, which contained 24 and 30 wt % MMA contents produced a significant decrease in the shear resistance results. This may in part be explained as a result of reduced interfacial wetting at the glass substrate due to reduced polymer mobility. As shown in Figure 3(a), the modulus of the PSAs increases with the MMA content, which results in the reduction in contact areas between the adhesive and substrate. Therefore, as the level of PMMA content was further increased, interfacial failure began to predominate and a reduction in shear resistance occurred.

The other important reason responsible for the increase of the shear resistance came from the microstructure of the dried lattices, i.e., the entanglement molecular weight, M_e. Chain entanglements behaved as pseudocrosslinks that eventually disentangled under shear stress but contributed to the measured shear resistance. It can be seen from the results of Table II that the decrease of the M_e resulted in the increase of the packing density of the molecular chains. Thus, a greater number of entanglements inhibits elongation and improves an adhesive's shear strength or holding power. Instead, these parameters characterize the intrinsic cohesive strength of the polymer, and qualitatively, the observed dependence on molecular weight reflects the increased resistance of the polymer to deformation due to the increasing viscosity and the increasing number of entanglements per molecule as M_w increases. Increasing cohesive strength thus made failure less likely to occur within the film itself. Shear strength is directly

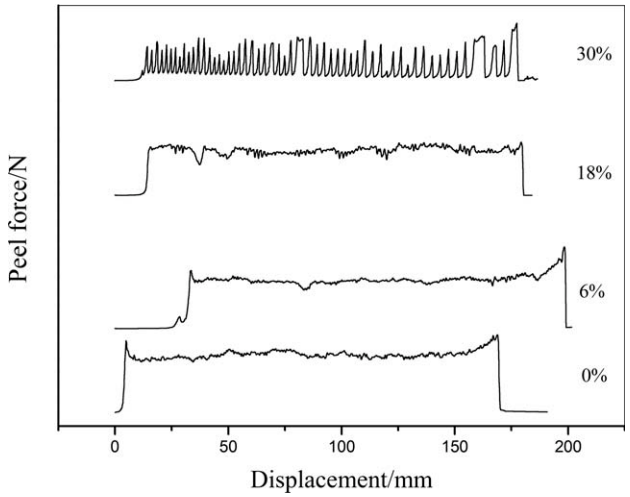

Figure 8 Force-displacement plot for the peel measurements(dwelling time = 24 h).

related to the zero-shear viscosity and the number of entanglements[22], so the increased number of entanglements at higher molecular weight logically corresponds to the increased shear holding power observed. Meanwhile, it must be noted that the intrinsic viscosity of the adhesive has to be able to properly wet the substrate. Therefore, copolymerizing the suitable concentration of the high T_g component and moderate molecular weight polymer played a significant role in influencing the shear resistance.[42]

Generally, an increase of cohesive strength causes a significant decrease of adhesion performances. Qu et al. reported that the latex with the smallest particle size gives the highest peel force. This is thought to be due to small particles being able to quickly conform to nanometer-scale roughness on the surface of the stainless steel plate, and thus increase the area of contact between the adhesive and the substrate. The larger particles require more time to accommodate to the surface roughness by polymer relaxation processes. At the longer adhesion time of 24 h, the peel force is slightly higher for the latex with the largest particle size.[30] The force measured during peel is composed of two components. Firstly, the force requires overcoming the work of adhesion, i.e., breaking the adhesive/substrate interfacial bond, and secondly the force requires deforming the bulk of the adhesive.[41,43] The peel is the outcome of the viscoelastic process. Zosel[44,45] showed that to achieve a high fracture energy during separation of the adhesive bond, the PSA had to form bridging fibrils, and the author remarked that these bridging fibrils could form only when the elastic modulus was below a certain value. Further studies by Lakrout et al.,[46] also on adhesives prepared from PEHA lattices, showed that the fibrils were actually walls between cavities, and finally an extensive study from the same group showed that these cavities expanded from defects at the interface between the adhesive and the rigid surface. Figure 7(b) shows the relationship between peel force and MMA content. From the results of Table III, the soluble polymers having broad polydispersity (MWD: 3.1–4.7) are effective in providing high viscoelastic energy dissipation during peeling. The increase in modulus (or decrease in polymer chain mobility) arising from copolymerization of MMA component in poly(BA-*co*-AA) resulted in a slightly lower peel adhesion at the 20-min test time due to reduced interfacial adhesion. An increase in adhesive modulus, shown in Figure 3(a), would decrease peel adhesion for two reasons. First, due to a decrease in the ability of the adhesive to wet the substrata, this eventually resulted in a polymer that had no pressure-sensitive properties. Secondly, as the modulus of the poly(BA-*co*-MMA-*co*-AA) increased the amount of adhesive filamentation at the locus decreased and hence the volume of adhesion under deformation decreased. The amount of filamentation at the locus of failure would decrease as the T_g (or modulus) of the copolymer increased. Further contributing factors to the decrease in peel adhesion as the MMA level increased were derived from a lowering in interfacial adhesion. This may be due to incomplete wetting of the substrate as a consequence of lower polymer mobility. A final increase in the level of PMMA to 30 wt % produced a film which dropped in peel force to nearly $1N/25$ mm. The large variation in peel adhesion was observed at the 24-h test time. Figure 8 shows graphically the relationship between the peel force and the displacement for the adhesives using the MMA contents as 0, 6, 18, and 30% in the separated forms. The failure for PSA films were the interfacial adhesion type, except for 30% MMA content, which showed the adhesion-slip failure. The increments in the proportion of MMA content produced a decrease of the fibrillation during the peeling process and a change in the mode of failure from cohesive to adhesive. An increase in the level of MMA content to 30 wt % produced a large reduction in forming elongated filaments, which significantly decreased peel energy (the viscoelastic dissipation).

Adhesive tack is a function of two factors: the ability of the adhesive to spread and wet the substrate, and the resistance of the adhesive to withdrawal. These are competing factors, since improving one generally has a negative effect on the other. A number of researches have been reported their results. Willenbacher focused on the effect of molecular weight on the adhesive behavior of a PSA, and investigated mixtures of low and high molecular weight PIB as model systems showing cavitation and fibrillation typical of PSAs.[47] The deformation of

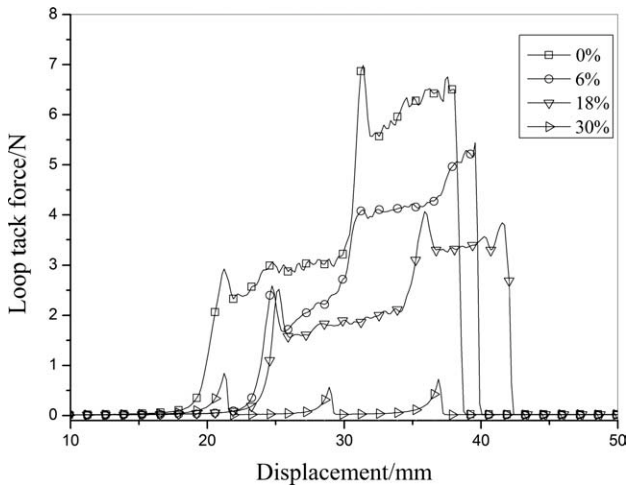

Figure 9 Force-displacement plot for the loop tack measurements.

an adhesive during probe withdrawal occurs in the following order: appearance of cavities on the probe surface; lateral growth of the cavities; and extensional growth of the cavities until fracture or debonding.[24,48] Many small cavities will appear, decreasing the load-bearing area. In a low-viscosity adhesive, growth of these voids occurs more easily and there are expected to be fewer, larger cavities.[49] As the cavities increase in volume, their internal pressure may become lower than the outside pressure, causing them to act like microscopic "suction cups,"[50] contributing to a greater work of adhesion. The different debonding and fibrillation characteristics are also illustrated by the video images obtained during tack tests. The fibrillation makes a significant contribution to the work of adhesion during the tack test. The work of adhesion W_{adh} is a function of the initial adhesion to the test probe as well as the ability of the PSA to dissipate energy during fibrillation and debonding.[43,51] During the debonding process two main mechanisms compete with each other: the propagation of cavities along the interface as cracks and the bulk expansion of the same cavities.[17] A thorough discussion of fibril growth is given by Creton in a recent publication.[52]

The major factor contributing to the reduction in loop tack as the level of MMA content increases, shown in Figure 7(c), is the increase in copolymer modulus. It is well known that the tack is inversely proportional to the elasticity modulus. Therefore, the loop tack force decreased with the increase of MMA content shown in Figure 3(a), and the response was more elastic during debonding. The strength of an adhesive bond is determined by the thermodynamic contributions to the interfacial energy (van der Waals interactions, electrostatic forces, and hydrogen bonding) and the rheological contributions due to the viscoelastic dissipation during deformation of the polymer chains in the adhesive layer itself. For example, air cavities impaired the strength of the adhesive bond by limiting contact. During contact between adhesive and the substrate, it could be assumed that there was some air trapped at the interface inside surface roughness as a consequence of lower loop tack. The nucleation of cavities under the influence of the tensile stress at the beginning of the debonding process and their growth is supposed to be the origin of fibrillation. Cavity becomes unstable and expands without limits above a critical dilatant stress, which is proportional to Young's modulus of the polymer and depends upon radius of the initial cracks. Fibrilation seemed to be crucial to the tack of polymers to be used as pressure-sensitive adhesives. For the high molecular weights from the soluble polymers, fibrillation increased the work of adhesion above that due to the contributions of good initial wetting and initial resistance to flow. The extent of fibrillation also depends on the strength of the interfacial adhesive bond. For a PSA with higher cohesive strength, the resistance to fibril elongation will rise more quickly, but its maximum value may depend on the interfacial bond with the substrate.

The results of the tack tests were loop tack force-displacement curves for the four PSA films with 0, 6, 18, and 30% MMA contents, as shown in Figure 9. Despite differences in the tack force-displacement curves, the picture patterns were rather similar, which implied a similar micromechanism of adhesive failure. The PSA films with low contents of MMA had reasonable tack properties, that is, acceptable wetting of the stainless panel during the contacting step and suitable tack force and tack energy during the debonding process. Suitable wetting was achieved during the bonding process when dissipation of energy in the bulk of the film was favored during the separation step. Therefore, to be effective, a PSA must be able to wet the surface with which it is brought into contact and low modulus-high elongation fibrils that are deformed during the debonding process. Hence, high visco-elastic energy dissipation could be obtained when there was good anchorage of the adhesive onto the substrate and low modulus-high elongation fibrils that were deformed during the debonding process. In conclusion, for optimum tack and adhesion, considered with the shear resistance, the well-balanced adhesive properties can be obtained from the incorporation of 18 wt % MMA content in poly(BA-*co*-AA).

CONCLUSIONS

Polyacrylic lattices with different MMA contents and narrow size distributions were successfully prepared by monomer-starved semicontinuous emulsion

polymerization. The six polymerizations produced coagulum levels of less than 0.5%, showing that the surfactant system used in this work produced stable lattices with high MMA contents. The measured and theoretical diameters of the latex particles during the polymerizations were in close agreement for all preparations. This provided a good indication that the polymerizations had occurred without a significant quantity of new particles being formed during the monomer feed. It was found that the average molecular weights of soluble polymer were increased as the MMA component increased, and the glass transitional temperature (T_g) of poly(BA-*co*-MMA-*co*-AA) linearly increased with the MMA content. Resistance to shear increased with increasing MMA content, but it suffered catastrophic failure at a fairly high MMA content. Meanwhile, the shear strength increased with the MMA content at the expense of lowering peel and tack. The lower tack and peel values might be attributed to the higher stiffness of the chains, which exerted in the wetting process of the substrate by the adhesive. The higher shear resistance may be correlate with the higher cohesion of the formed microsphers as the consequence of the higher T_g values. The decrease in peel adhesion and tack with the MMA content was attributed to a reduction in the ability of the adhesive to wet the substrate. The amount of filamentation at the locus of failure would have decreased as the T_g of the copolymer increased.

References

1. Benedek, I.; Heymans, L. J. Pressure-Sensitive Adhesives Technology; Marcel Dekker: New York, 1997.
2. Laureau, C.; Vicente, M.; Barandiaran, M. J.; Leiza, J. R.; Asua, J. M. J Appl Polym Sci 2001, 81, 1258.
3. Wang, C. L.; Wang, L.; Chen, C.; Chen, T.; Jiang, G. H. J Appl Polym Sci 2006, 101, 1535.
4. Staicu, T.; Micutz, M.; Leca, M. Prog Org Coat 2005, 53, 56.
5. Demarteau, W.; Loutz, J. M. Prog Org Coat 1996, 27, 33.
6. Roberge, S.; Dube, M. A. Polymer 2006, 47, 799.
7. Jovanovic, R.; Ouzineb, K.; McKenna, T. F.; Dube M. A. Macromol Symp 2004, 206, 43.
8. Chu, H.-H.; Lee, C.-M.; Huang, W. G. J Appl Polym Sci 2004, 91, 1396.
9. Parouti, S.; Kammona, O.; Kiparissides, C.; Bousquet, J. Polym React Eng 2003, 11, 829.
10. Canche-Escamilla, G.; Mendizabal, E.; Hernandez-Patino, M. J.; Arce-Romero, S. M.; Gonzalez-Romero, V. M. J Appl Polym Sci 1995, 56, 793.
11. Gonzalez, I.; Asua, J. M.; Leiza, J. R. Polymer 2007, 48, 2542.
12. Jiang, S.; Sudol, E. D.; Dimonie, V. L.; El-aasser, M. S. J Polym Sci A Polym Chem 2007, 45, 2105.
13. Chern, C. S.; Hsu, H. J Appl Polym Sci 1995, 55, 571.
14. Yurekli, Y.; Altinkaya, S. A.; Zielinski, J. M. J Polym Sci B Polym Phys 2007, 45, 1996.
15. Jovanovié, R.; Dubé, M. A. J Macromol Sci Polym Rev 2004, 44, 1.
16. Aymonier, A.; Leclercq, D.; Tordjeman, P.; Papon, E.; Villenave, J.-J. J Appl Polym Sci 2003, 89, 2749.
17. Amaral, M. D.; Roos, A.; Asua, J. M.; Creton, C. J Colloid Interf Sci 2005, 281, 325.
18. Kajtna, J.; Likozar, B.; Golob, J.; Krajnc, M. Int J Adhes Adhes 2008, 28, 382.
19. Aymonier, A.; Papon, E.; Villenave, J.-J.; Tordjeman, P.; Pirri, R.; Gerard, P. Chem Mater 2001, 13, 2562.
20. Marcais, A.; Papon, E.; Villenave, J.-J. Macromol Symp 2000, 151, 497.
21. Cannon L. A.; Pethrick, R. A. Macromolecules 1999, 32, 7617.
22. Singa, D. T.; Andew, K. J Appl Polym Sci 2001, 79, 2230.
23. Gower, M. D.; Shanks, R. A. J Polym Sci B Polym Phys 2006, 44, 1237.
24. Wang, T.; Lei, C.; Dalton, A. B.; Creton, C.; Lin, Y.; Fernando, K. A. S.; Sun, Y.; Manea, M.; Asua, J. M.; Keddie, J. L. Adv Mater 2006, 18, 2730.
25. Tobing, S. D.; Klein, A. J Appl Polym Sci 2001, 79, 2558.
26. Ghosh, S.; Krishnamurti, N. Eur Polym Mater 2000, 36, 2125.
27. Lovell, P. A.; Shah, T. H. Polym Commun 1991, 32, 98.
28. Chauvet, J.; Asua, J. M.; Leiza, J. R. Polymer 2005, 46, 9555.
29. Chevalier, Y.; Hidalgo, M.; Cavaille, J.-Y.; Cabane, B. Macromolecules 1999, 32, 7887.
30. Qu, X.; Wang, N.; Lovell, P. A. J Appl Polym Sci 2009, 112, 3030.
31. Wang, N.; Guo, Y.; Xu, H.; Liu, X.; Zhang, L.; Qu, X.; Zhang, L. J Appl Polym Sci 2009, 113, 3113.
32. Shen, H.; Zhang, J.; Liu, S.; Liu, G.; Zhang, L.; Qu, X. J Appl Polym Sci 2008, 107, 1793.
33. Plessis, C.; Arzamendi, G.; Leiza, J. R.; Alberdi, J. M.; Schoonbrood, H. A. S.; Charmot, D.; Asua, J. M. J Polym Sci A Polym Chem 2001, 39, 1106.
34. Mayer, A.; Pith, T.; Hu, G. H.; Lambla, M. J Polym Sci B Polym Phys 1995, 33, 1781.
35. Jovanovic, R.; McKenna, T. F.; Dube, M. A. Macromol Mater Eng 2004, 289, 467.
36. Sayer, C.; Lima, E. L.; Pinto, J. C.; Arzamendi, G.; Asua, J. M. J Polym Sci A Polym Chem 2000, 38, 1100.
37. Elizalde, O.; Leiza, J. R.; Asua, J. M. Ind Eng Chem Res 2004, 43, 7401.
38. Hutchinson, R. A.; McMinn, J. H.; Paquet, D. A.; Beuermann, S.; Jackson, C. Ind Eng Chem Res 1997, 36, 1103.
39. Lovell, P. A.; El-Aasser Mohamed, S. Emulsion Polymerization and Emulsion Polymers; Wiley: Chichester, 1997, p 624.
40. Tobing, S.; Klein, A.; Sperling, L. H.; Petrasko, B. J Appl Polym Sci 2001, 81, 2109.
41. Yang, H. W. H. J Appl Polym Sci 1995, 55, 645.
42. Kajtna, J.; Likozar, B.; Golob, J.; Krajnc, M. Int J Adhes Adhes 2008, 28, 382.
43. Zosel, A. Int J Adhes Adhes 1998, 18, 265.
44. Zosel, A. Colloid Polym Sci 1985, 263, 541.
45. Zosel, A. Int J Adhes Adhes 1998, 18, 265.
46. Lakrout, H.; Sergot, P.; Creton, C. J Adhes 1999, 69, 307.
47. O'Connora, A. E.; Willenbacher, N. Int J Adhes Adhes 2004, 24, 335.
48. Lakrout, H.; Creton, C.; Ahn, D.; Shull, K. R. Macromolecules 2001, 34, 7448.
49. Gay, C.; Leibler, L. Phys Today 1999, 52, 48.
50. Gay, C.; Leibler, L. Phys Rev Lett 1999, 82, 936.
51. Urahama, Y. J Adhes 1989, 31, 47.
52. Creton, C. Mater Sci Technol 1997, 18, 708.